Proceedings of the Canadian Society for Mechanical Engineering International Congress
32nd Annual Conference of the Computational Fluid Dynamics Society of Canada
Canadian Society of Rheology Symposium
CSME-CFDSC-CSR 2025
May 25–28, 2025, Montréal, Québec, Canada

Empirical Quantification of Uncertainty in iGPS Measurements for Assembly Operations

Moloud Jafari[1*], Sasan Sattarpanah Karganroudi[2], Louis Rivest[3], Souheil Antoine Tahan[1]
[1]Département de génie mécanique, École de Technologie Supérieure (ÉTS), Montréal, Canada
[2]Département de génie mécanique, Université du Québec à Trois-Rivières (UQTR), Trois-Rivières, Canada
[3]Département de génie des systèmes, École de Technologie Supérieure (ÉTS), Montréal, Canada
*Moloud.jafari.1@ens.etsmtl.ca

Abstract—Jigless assembly is a flexible and cost-efficient alternative to traditional jig-based methods in mid and large-scale manufacturing. Accurate metrology systems, such as Indoor GPS (iGPS) offers us a technological opportunity to achieve this type of assembly while guaranteeing flexibility and precision. This study proposes a methodology for empirical estimation for measurement uncertainties at one single point within a predefine work volume, inherent in the use of iGPS, following GUM guidelines. The methodology involves identifying primary uncertainty sources, including equipment errors, repeatability, and references used for the calibration. Experiments were conducted using an artefact bar calibrated by an Absolute Laser Tracker AT960, with statistical analysis performed to quantify the impact of calibration, warm-up time, and measurement distance. The findings contribute to understanding iGPS capabilities and offer practical insights for optimizing measurement strategies in jigless assembly, enhancing precision and efficiency in large-scale manufacturing environments.

Keywords-component; Jigless Assembly; Indoor GPS (iGPS); Measurement Uncertainty; Large-Scale Metrology; Metrology-Assisted Assembly(MAA)

I. INTRODUCTION

In medium and large-scale industries, production costs across various stages, particularly in design and assembly, increase significantly due to the massive scale of production. Ensuring accurate assembly is critical, as any deviation can impact product performance and safety [1]. Traditionally, jigs have been employed to ensure accurate positioning and stability during assembly, but they introduce high costs, limited flexibility, and inefficiencies, particularly in low-rate production environments [2].

Jigless assembly has emerged as an attractive alternative, relying on precise component manufacturing to reduce tooling costs and enhance adaptability [3]. However, achieving accurate alignment without jigs poses challenges, necessitating the use of advanced metrology systems. Large-Scale Metrology (LSM) provides essential measurements for such assembly processes, but issues related to calibration, uncertainty evaluation, and system integration persist [4].

Modern large-scale dimensional measurement systems, such as laser trackers and indoor GPS (iGPS), are designed to capture absolute three-dimensional coordinates. Consequently, verifying the metrological performances of these systems through calibration measurements alone is insufficient to ensure the traceability of all coordinate data. While direct comparison of coordinate measurements has emerged as a promising approach, establishing reliable and calibrated reference coordinates in large-scale environments remains a significant challenge [5].

iGPS system offers a promising solution with its large-area coverage, mobility, and precision. Utilizing rotating laser signals and sensors for triangulation, iGPS is well suited for aerospace applications but is subject to uncertainties from equipment, environment, and references [6]. Estimating these uncertainties is vital for ensuring measurement reliability.

This paper focuses on estimating the expanded uncertainties (U_X, U_Y, U_Z) at one single point (P) within a work volume, inherent in the use of iGPS. These uncertainties should include equipment error, repeatability and reference error in accordance with the Guide to the Expression of Uncertainty in Measurement (GUM). A structured methodology is presented to identify uncertainty sources, conduct controlled experiments, and validate results, contributing to improved reliability of iGPS in jigless assembly

II. BACKGROUND AND RELATED WORK

In the past, particularly in large-scale aerospace assemblies, skilled craftsmen manually positioned parts using general tools. However, this method proved inefficient, leading to the use of rigid and costly jigs. Despite advancements in engineering and technology within the aerospace industry, the use of such jigs

persists due to the difficulty of maintaining tight tolerances in large structures. Precise alignments, particularly in drilling patterns, are challenging to achieve, and the common solution has been the use of jigs during assembly. However, this reliance on jigs introduces limitations such as reduced flexibility and lower production efficiency[7].

According to Mello et al. [2] production flexibility was successfully increased by utilizing a Universal Magnetic Table (UMT) and lean manufacturing in a robotic cell for aircraft assembly. However, the process still faces challenges such as the need for skill development and training, as well as establishing effective human-machine interaction. It highlights the significant role of automation in jigless assembly, demonstrating that it can reduce labor costs by 50-80% and lower overall product costs by 25-75%. To achieve successful automation, it is crucial to design products with automation as a key consideration.

Mozzillo et al. [3] investigated jigless assembly in aeronautical structures, demonstrating cost reduction and improved precision through ergonomic analysis, digital modeling, and statistical tolerance prediction. While their virtual simulations showed promising results, they emphasized the need for real-world validation. Fukuda et al. [8] developed a jigless robotic assembly method using a self-aligning robotic hand, achieving high accuracy without traditional jigs, particularly beneficial for small- and medium-scale productions. However, limited adaptability to diverse part shapes highlighted the need for further research. Fiedler et al. [1] proposed integrating jig features directly into automotive parts to reduce fixture costs and improve production flexibility, though the concept remains in its early stages and requires further development for large-scale applications.

The need for control systems in jigless assembly arises from the challenge of maintaining precise alignment and positioning without relying on fixed jigs. In such systems, real-time adjustments are crucial to ensure accuracy throughout the assembly process. These systems play an essential role by enhancing part alignment and enabling continuous adjustments as assembly progresses. Additionally, they are fundamental to adapting jigless assembly within Industry 4.0 environments, where data integration and automation are key. Moreover, incorporating digital twin simulations and artificial intelligence (AI) within control systems can predict maintenance needs and optimize workflows, effectively substituting for the precision traditionally provided by physical jigs. In summary, control systems play a critical role in jigless assembly by compensating for the absence of traditional jigs, providing flexibility, precision, and seamless integration with advanced manufacturing processes [9]. They are essential for enhancing assembly efficiency and adaptability, while meeting the demanding accuracy requirements of industries such as aerospace and automotive [10].

3D Metrology-Assisted Assembly (MAA) is an advanced assembly method that utilizes real time 3D metrology capabilities to monitor critical dimensional and geometric features during tooling and assembly processes. By using precise dimensional measurements to guide assembly operations, MAA enhances process efficiency and economic performance. To meet quality management standards, MAA requires metrological traceability through uncertainty analysis and capability studies, ensuring accurate and reliable assembly from the outset [11].

The iGPS system is an advanced coordinate measurement tool that operates over large areas without a conventional frame, using laser signal transmitters and sensors to determine azimuth and elevation angles [6]. While iGPS offers precision and flexibility in large-scale industrial applications, particularly in aerospace and robotics, challenges related to accuracy, integration, and dynamic performance remain.

Several studies have explored these challenges. Drouot et al. [12] focused on improving assembly accuracy in aerospace applications but highlighted the difficulty of balancing accuracy and efficiency in large-scale production. Han et al. [13] aimed to enhance iGPS's dynamic performance in industrial robots, though integration with other systems remained challenging. Ferri et al. [14] developed statistical models to optimize iGPS settings, reducing uncertainty but lacking real-world validation and comprehensive cost-benefit analysis. Tang and Chen improved measurement accuracy in digital manufacturing using iGPS but identified a need for further integration with emerging technologies like AI [15]. Ren et al. [5] optimized iGPS tracker placement using genetic algorithms, reducing uncertainty but leaving environmental and dynamic challenges unexplored. Wang et al. [16] improved iGPS dynamic performance with new software, though bias errors persisted in complex conditions and at high speeds.

Further research has explored the potential of hybrid and simulated approaches to improve iGPS performance. Muelaner et al. [6] validated iGPS accuracy by comparing its measurements with laser tracker data and applying Monte Carlo simulations to assess uncertainty. Although the system performed well with 95% confidence ($\pm 2\sigma$), additional real-world testing and long-term assessments were recommended. Zhao et al. [17] integrated iGPS and laser tracker systems to align aerospace structures, achieving high measurement accuracy despite challenges with error propagation and calibration complexity. Similarly, Nicksch et al. [18] developed a virtual iGPS model to predict measurement uncertainty and optimize transmitter placement, reducing uncertainty but emphasizing the need for further validation in practical assembly environments.

These studies highlight advancements in reducing uncertainty and enhancing the performance of the iGPS system. However, challenges persist, such as assessing the uncertainty related to the iGPS device, evaluating how uncertainty propagates in 3D space, improving integration with other systems, and achieving real-world validation. These unresolved issues require further research a more in-depth examination of uncertainty and its implications in the upcoming section.

III. METHODOLOGY

As previously mentioned, this study focuses on estimating the measurement uncertainties (U_X, U_Y, U_Z) of the iGPS system at a single point (P) within a defined work volume, following Guide to the Expression of Uncertainty in Measurement (GUM) guidelines [19]. The following methodology outlines the steps taken to achieve this.

The process begins with the identification and categorization of all potential sources of uncertainty in iGPS measurements. These sources encompass environmental factors, reference-based deviations, and system-related errors. Controlled experiments, including calibration and repeatability tests, are conducted to quantify these uncertainties at the selected point in 3D space. The results are then validated through practical testing and comparisons with real-world iGPS measurements to ensure the robustness of the findings. The analysis follows the ASME Y14.5 standard for defining dimensional and geometric requirements, while the uncertainty evaluation follows ISO 10360 CMM standards [20], [21]. To ensure measurement stability, systems will be powered on one hour before use. Additionally, the iGPS will be calibrated before each test, as recommended, to maintain measurement accuracy.

A) Measuring Equipment

This study utilizes two advanced measurement systems: the Absolute Laser Tracker AT960, developed by Leica Geosystems, and the 7D Kinematic Metrology iGPS system. The AT960, with 6 degrees of freedom (6DoF), provides high-precision measurements with a Maximum Permissible Error (MPE) of ±15µm +6 µm/m, using PolyWorks® software [22]. The iGPS system employs six transmitters to track reflective targets with a precision of ± 200µm + 20µm/m at a 95% confidence level, using Surveyor® software [23].

B) Development of a Measurement System

A reference bar is used as the primary artifact. This bar is equipped with additional attachments that allow it to be positioned at 90° and 45° angles. These attachments, when connected, transform the bar into a triangular structure, facilitating its alignment with vertical and diagonal planes (Figure 1). This configuration ensures better coverage of measurement orientations, particularly for diagonal and functional surfaces. The reference bar measures 2294.99 mm and is divided into eight sections.

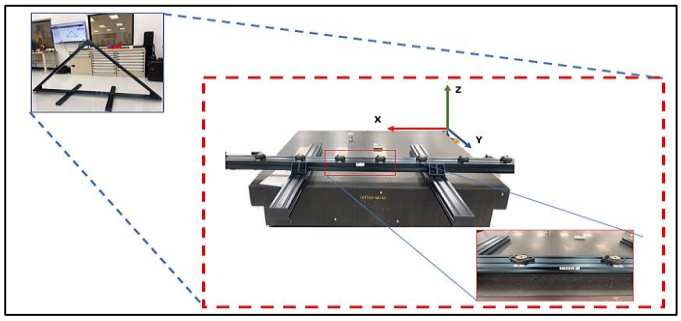

Figure 1: iGPS Measurement System

The measurement function calculates the distance between two points by determining the absolute value of their vector components, as shown in Equation 1, where $\vec{r}_i$ and $\vec{r}_j$ represent the position vectors of points *i* and *j* in 3D space:

$$d = \left|\vec{r}_i - \vec{r}_j\right| \tag{1}$$

For simplicity, this process is first explained using two points, though the actual measurement will involve eight points. The Euclidean distance $d_{ij}(\mathbb{R}^6 \rightarrow \mathbb{R}_+)$ between two points in three-dimensional space based on their coordinates, as presented in Equation 2. Here, x_i, y_i, z_i and x_j, y_j, z_j are the spatial coordinates of points *i* and *j*, respectively.

$$d_{ij} = \sqrt{(x_i - x_j)^2 + (y_i - y_j)^2 + (z_i - z_j)^2} \tag{2}$$

Tests are conducted in a controlled laboratory environment at LIPPS Labo (Montréal, ÉTS), where the temperature is maintained at 20±1°C. This process is repeated in the same manner for every point.

C) Laser Tracker Uncertainty Calculation and iGPS Reference Bar Calibration

To calibrate the reference bar, a laser tracker (Absolute Laser Tracker 960) was used, as illustrated in Figure 2a. Multiple measurements were taken to minimize random and environmental errors, using this device, which is known for its superior accuracy compared to the iGPS. In order to minimize operational errors, the reference bar was positioned in front of the laser tracker. Random points were selected on the bar, and the Euclidean distance between these points was calculated using Equation 2. This approach eliminates the need for coordinate system alignment, allowing direct comparisons between the laser tracker and iGPS data, regardless of their reference systems. The estimation of laser tracker uncertainty involves several steps to ensure accurate distance measurements. First, according to GUM, the standard uncertainties are determined, considering measurement reference, resolution, equipment error, and repeatability uncertainties. Equipment error uncertainty which increases with distance from the laser tracker is derived from the Maximum Permissible Error (MPE), specified as ±15µm+6µm/m and converted to a standard deviation using division by √3, assuming a rectangular distribution. The uncertainty analysis involved multiple steps: calculating the mean coordinates, determining the standard deviation, and estimating the standard error for each coordinate. Repeatability uncertainty is assessed through recurring measurements. Next, the standard uncertainty is calculated, followed by the computation of the combined standard uncertainty, which serves as a reference for future iGPS measurements.

To account for environmental variations, such as temperature fluctuations, measurements were repeated over three consecutive days, with three repetitions each day. The Euclidean distances between identical points recorded across different days were compared, and the mean distance was calculated to improve result reliability. Finally, the worst-case scenario, the maximum uncertainty value was selected as the reference uncertainty for the iGPS system, as described in Equation 3.

$$U_{Final} = max\ (U_{di}) \quad (3)$$

Since iGPS lacks a specific standard, the ISO 10360 CMM standards was applied as a guideline to ensure measurement reliability. Calibration procedures provided by the iGPS manufacturer were meticulously followed, including maintaining a consistent walking pace during the calibration process, tilting the calibration scale bar, recording at least 10 reference points per transmitter, and avoiding reflective surfaces to prevent measurement distortions. This systematic calibration ensures accurate and reliable uncertainty estimation for subsequent iGPS measurements.

The iGPS measurement process was conducted using G6 detectors at eight reference points after a one-hour warm-up period, as shown in Figure 2b. Over three consecutive days, measurements were taken immediately after the calibration and again 4 and 5 hours later to evaluate the impact of warm-up time and calibration on measurement accuracy. The Euclidean distances were calculated and compared with the corresponding measurements obtained using the laser tracker.

A one-way ANOVA analysis was applied to assess the effects of calibration time, warm-up intervals, and measurement distance on measurement uncertainty. The ANOVA results, including group means, F statistics, and p -values, were analyzed to determine whether these factors had a statistically significant impact on the iGPS measurements.

To calculate iGPS uncertainty, the same procedure used for the laser tracker was applied. The standard uncertainty was derived by combining equipment, reference devices, and reproducibility uncertainties using the Taylor series expansion and the law of uncertainty propagation, as shown in Equation 4:

$$u_d = \sqrt{\left[\frac{\partial f}{\partial x_i}\, u(x_i)\right]^2 + \cdots + \left[\frac{\partial d}{\partial z_j}\, u(z_j)\right]^2} \quad (4)$$

The combined uncertainty was calculated independently for each axis, assuming no correlation between the X, Y, and Z components. Finally, the maximum uncertainty value across all measured distances was reported as the final uncertainty, ensuring a conservative estimate of the system's measurement accuracy within the work volume.

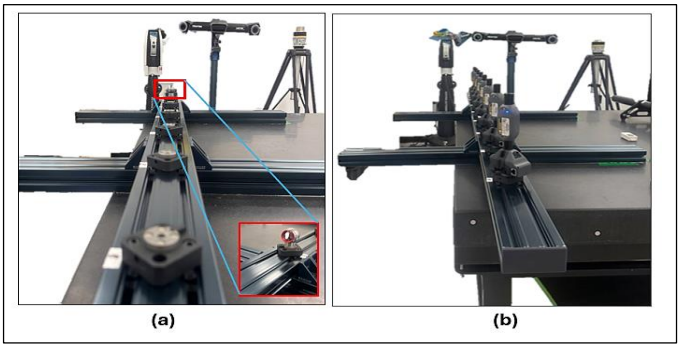

Figure 2: a) Measurement of the reference bar with the Absolute Laser Tracker 960 for Calibration b) Measurement of the reference bar with the iGPS.

IV. Results

A) Analysis of Measurement Uncertainty as a Function of Distance

Figure 3 shows the uncertainty of points measured by the laser tracker based on their average distance from the device. As shown in the graph, uncertainty increases with distance. The x-axis represents the distance from the laser tracker, while the y-axis indicates the combined uncertainty $u_{x_{point}}$ in millimeters. The maximum uncertainty, $u_{max_{LT}} = 0.0325\ mm$, occurs at the farthest distance, emphasizing the need for stable conditions and proper calibration.

B) iGPS Uncertainty Measurement and Bias Analysis

In the following section, the measurement uncertainty of the iGPS system is analyzed. As described in the methodology section, the iGPS uncertainty was determined using the laser tracker as the reference device.

This analysis considers two categories: (1) random error, including repeatability uncertainty from tests and data, instrument uncertainty from the iGPS manufacturer, and reference device uncertainty from laser tracker measurements; and, (2) systematic error (bias), arising from the difference between iGPS and laser tracker measurements.

To examine the factors influencing systematic errors, multiple analyses were conducted to assess the impact of various variables. This was done with the aim of calculating systematic uncertainty or bias, and this process included the analysis of potential influencing factors such as calibration effects, warm-up time, and distance between measurement points. To ensure measurement consistency, all iGPS measurements were performed under the same settings and conditions. The process was repeated over three consecutive days, with three repetitions each day. To assess the statistical significance of these factors, standard deviations and means were calculated, and a one-way ANOVA analysis was performed using Minitab software. This analysis provided insights into the impact of these factors on iGPS measurement uncertainty, supporting the overall evaluation of the system's performance.

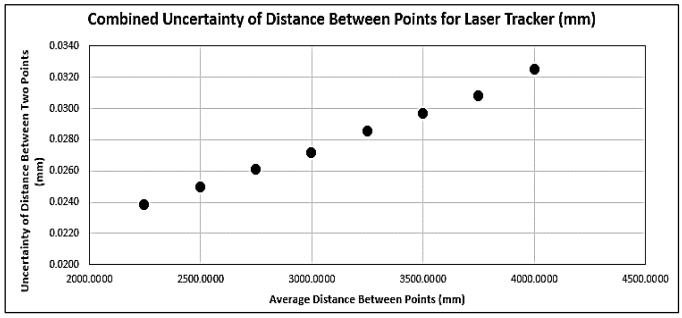

Figure 3: Combined uncertainty of laser tracker measurements versus distance

C) ANOVA Analysis of iGPS Uncertainty Under Different Conditions

1. Calibration Effects

The one-way ANOVA analysis for calibration effects shows a F-value of 2.29 and a p-value of 0.107. Since the P-value

exceeds the 0.05 threshold, there is no statistically significant difference in measurement uncertainty to calibration. This suggests that performing the calibration process over three consecutive days does not impact the measurement results. The Tukey test results in Figure 4 confirm this, as all confidence intervals include zero, indicating consistency in the calibration process.

2. Warm-Up Time

The impact of warm-up time on measurement uncertainty is illustrated in Figure 5. The ANOVA analysis shows an F −value of 1.28 and a p-value of 0.284. As this p-value is greater than 0.05, no significant variation is detected between measurements taken directly after calibration and those taken within 4 and 5 hours of calibration. The Tukey test in Figure 5 shows overlapping confidence intervals, reinforcing the stability of the iGPS system over the tested time intervals. The analysis suggests that even after 5 hours post-calibration, the iGPS system maintains its accuracy, with no noticeable deviations in measurement results. This demonstrates the system's reliable performance across extended time periods.

3. Distance Between Points

The ANOVA results for the distance factor reveals a F-value of 8.70 and a p-value near 0.000, which is below the 0.05 threshold. This indicates a statistically significant effect of distance on measurement uncertainty. The Tukey test results in Figure 6 further confirm this by displaying distinct confidence intervals for various distance comparisons. Increased distances between points elevate uncertainty, impacting measurements in both the iGPS and laser tracker systems. The most significant factor affecting measurement results was the distance between points. As the distance increased, so did the uncertainty, impacting measurements in both the iGPS and laser tracker systems.

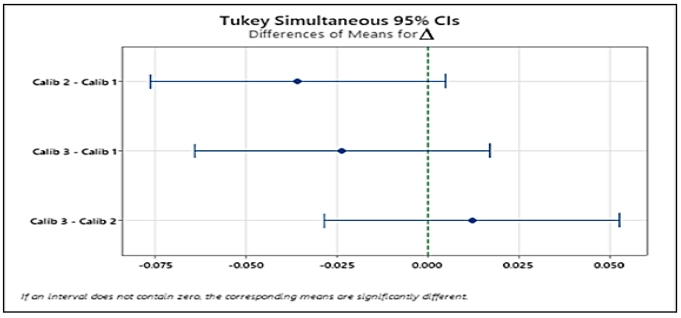

Figure 4: Effect of repeated calibrations on uncertainty

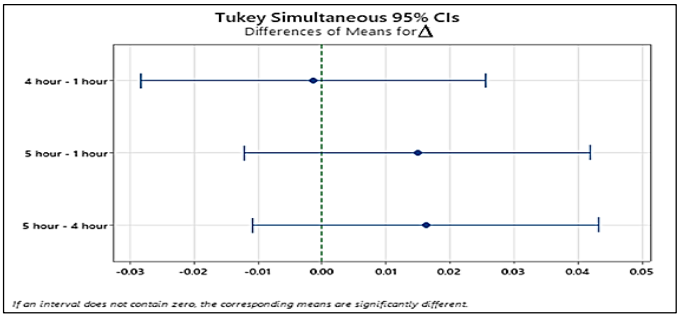

Figure 5: Effect of warm-up time on uncertainty

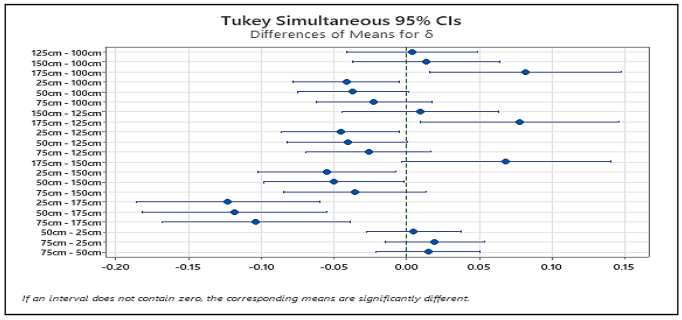

Figure 6: Distance effect on uncertainty

D) Analysis of iGPS Measurement Uncertainty

According to our experimental results, the most influential factor affecting measurement uncertainty was the distance between measured points. In contrast, repeated calibrations and warm-up time had negligible effects and were not statistically significant. Therefore, the analysis focused on the impact of distance.

The systematic error (bias) was calculated as the average difference between iGPS and laser tracker measurements. This procedure was repeated over three consecutive days, with three repetitions each day. The resulting bias was 0.440 mm.

The random error was estimated by summing the square of each individual uncertainty component, including repeatability, instrument, and reference uncertainties and then taking the square root of the total. The methodology for calculating each component is detailed in the Methodology section.

For this analysis, uncertainty values were calculated for each measurement point along the X, Y, and Z axes. Then, for each Euclidean distance between two points, the associated uncertainty was calculated by combining the uncertainties of those two points along each axis.

To ensure full spatial coverage of the defined working volume above the Metrology Granite Table, measurements were performed in all three main directions (X, Y, and Z). The experimental setups and example configurations are shown in Figure 7. As illustrated, the layout was planned to cover the entire workspace, and the results from each axis were compared. Although only one setup per direction is shown in the figure, similar measurements were repeated at different positions to fully cover the volume.

For each axis, measurements were performed along multiple directions (two for X, two for Y, and four for Z). For each direction, Euclidean distances were measured, and their associated combined uncertainties were calculated. The maximum combined uncertainty value among all directions for a given axis was selected as the representative uncertainty for that axis.

Expanded uncertainties were calculated by applying a coverage factor of 2, corresponding to a 95% confidence level. The final results showed consistent and stable measurement uncertainties across all three axes:

X-axis: U_X= 0.4985 mm

Y-axis: U_Y= 0.5182 mm

Z-axis: U_Z= 0.4992 mm.

These results are in strong agreement with theoretical expectations, confirming the robustness and reliability of the iGPS system within the defined workspace.

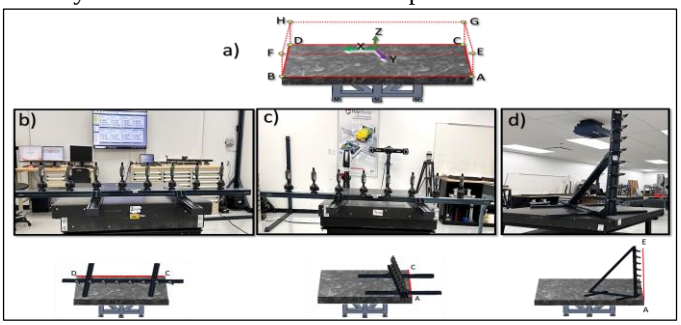

Figure 7: Representative measurement configurations for each axis to evaluate iGPS uncertainty along the X, Y, and Z directions (a) Schematic overview of the defined working volume on the Metrology Granite Table. (b–d) Selected configurations for X, Y, and Z directions, each showing both the real laboratory setup and its schematic view.

V. CONCLUSIONS

This study successfully analyzed the uncertainties of one single measurement point within a work volume, inherent in the use of iGPS using GUM guidelines. The findings highlight the significance of distance as a primary factor influencing measurement uncertainty, while calibration and warm-up times had negligible effects. The experimental results demonstrate the reliability and precision of iGPS for jigless assembly applications in large-scale manufacturing. These findings can be useful in fixtureless assembly optimization and improving accuracy in the aerospace and automotive industries.

REFERENCES

[1] F. Fiedler *et al.*, "Jigs and Fixtures in Production: A Systematic Literature Review," *J. Manuf. Syst.*, vol. 72, pp. 373–405, Feb. 2024, doi: 10.1016/j.jmsy.2023.10.006.

[2] J. M. G. de Mello, L. G. Trabasso, A. C. Reckevcius, A. L. O. A. Palmeira, P. Reiss, and W. Caraca, "A novel jigless process applied to a robotic cell for aircraft structural assembly," *Int. J. Adv. Manuf. Technol.*, vol. 109, no. 3, pp. 1177–1187, Jul. 2020, doi: 10.1007/s00170-020-05700-4.

[3] R. Mozzillo, P. Iaccarino, F. Vitolo, and P. Franciosa, "Design and development of jigless assembly process: the case of complex aeronautical systems," in *2019 II Workshop on Metrology for Industry 4.0 and IoT (MetroInd4.0&IoT)*, Jun. 2019, pp. 132–136. doi: 10.1109/METROI4.2019.8792874.

[4] R. H. Schmitt *et al.*, "Advances in Large-Scale Metrology – Review and future trends," *CIRP Ann.*, vol. 65, no. 2, pp. 643–665, Jan. 2016, doi: 10.1016/j.cirp.2016.05.002.

[5] Y. Ren, Y. Fu, F. Liu, and F. Zhang, "Multilateration with laser tracker applied in large-scale coordinate calibration," in *Optical Metrology and Inspection for Industrial Applications VI*, SPIE, Nov. 2019, pp. 107–113. doi: 10.1117/12.2539646.

[6] J. E. Muelaner, Z. Wang, J. Jamshidi, and P. G. Maropoulos, "Verification of the Indoor GPS System by Comparison with Points Calibrated Using a Network of Laser Tracker Measurements," in *Proceedings of the 6th CIRP-Sponsored International Conference on Digital Enterprise Technology*, G. Q. Huang, K. L. Mak, and P. G. Maropoulos, Eds., Berlin, Heidelberg: Springer, 2010, pp. 607–619. doi: 10.1007/978-3-642-10430-5_47.

[7] J. E. Muelaner, A. Kayani, O. Martin, and P. Maropoulos, "Measurement Assisted Assembly and the Roadmap to Part-To-Part Assembly: 7th International Conference on Digital Enterprise Technology," Sep. 2011, pp. 11–19. Accessed: Oct. 16, 2024. [Online]. Available: http://www.lms.mech.upatras.gr/DET2011/

[8] T. Fukuda, H. Dobashi, H. Nagano, Y. Tazaki, R. Katayama, and Y. Yokokohji, "Jigless assembly of an industrial product by a universal robotic hand mounted on an industrial robot," *Robotica*, vol. 41, no. 8, pp. 2464–2488, Aug. 2023, doi: 10.1017/S0263574723000474.

[9] G. Schuh, G. Bergweiler, M. V. Chougule, and F. Fiedler, "Effects of Digital Twin Simulation Modelling on a Flexible and Fixtureless Production Concept in Automotive Body Shops," *Procedia CIRP*, vol. 104, pp. 768–773, 2021, doi: 10.1016/j.procir.2021.11.129.

[10] M. Dalle Mura and G. Dini, "Augmented Reality in Assembly Systems: State of the Art and Future Perspectives," in *Smart Technologies for Precision Assembly*, S. Ratchev, Ed., Cham: Springer International Publishing, 2021, pp. 3–22. doi: 10.1007/978-3-030-72632-4_1.

[11] J. E. Muelaner, O. C. Martin, and P. G. Maropoulos, "Achieving Low Cost and High Quality Aero Structure Assembly through Integrated Digital Metrology Systems," *Procedia CIRP*, vol. 7, pp. 688–693, Jan. 2013, doi: 10.1016/j.procir.2013.06.054.

[12] A. Drouot, R. Zhao, L. Irving, D. Sanderson, and S. Ratchev, "Measurement Assisted Assembly for High Accuracy Aerospace Manufacturing∗," *IFAC-Pap.*, vol. 51, no. 11, pp. 393–398, Jan. 2018, doi: 10.1016/j.ifacol.2018.08.326.

[13] R. Han, T. Dunker, E. Trostmann, and Z. Xu, "Research on high-precision tracking and localization of industrial robots based on iGPS," *Meas. Sci. Technol.*, vol. 35, no. 6, p. 065006, Mar. 2024, doi: 10.1088/1361-6501/ad2f08.

[14] C. Ferri, L. Mastrogiacomo, and J. Faraway, "Sources of variability in the set-up of an indoor GPS," *Int. J. Comput. Integr. Manuf.*, vol. 23, no. 6, pp. 487–499, Jun. 2010, doi: 10.1080/09511921003642147.

[15] X. Tang and Z. Chen, "A Multi-dimensional Model for Computer-Aided Measuring Planning (CAMP) in Digital Manufacturing," in *Knowledge Discovery, Knowledge Engineering and Knowledge Management*, A. Fred, J. L. G. Dietz, K. Liu, and J. Filipe, Eds., Berlin, Heidelberg: Springer, 2015, pp. 56–65. doi: 10.1007/978-3-662-46549-3_4.

[16] Z. Wang, L. Mastrogiacomo, F. Franceschini, and P. Maropoulos, "Experimental comparison of dynamic tracking performance of iGPS and laser tracker," *Int. J. Adv. Manuf. Technol.*, vol. 56, no. 1, pp. 205–213, Sep. 2011, doi: 10.1007/s00170-011-3166-0.

[17] G. Zhao, P. Zhang, and W. Xiao, "Coordinate alignment of combined measurement systems using a modified common points method," *J. Instrum.*, vol. 13, no. 03, p. P03021, Mar. 2018, doi: 10.1088/1748-0221/13/03/P03021.

[18] C. Nicksch, M. Sabzehi, and R. H. Schmitt, "Virtual indoor-GPS for measurement uncertainty determination in reconfigurable environments," *Prod. Eng.*, vol. 16, no. 4, pp. 545–560, Aug. 2022, doi: 10.1007/s11740-022-01111-4.

[19] "JCGM - Joint Committee for Guides in Metrology." Accessed: Oct. 16, 2024. [Online]. Available: https://www.iso.org/sites/JCGM/GUM-introduction.htm

[20] "Y14.5 Dimensioning and Tolerancing - ASME." Accessed: Feb. 16, 2025. [Online]. Available: https://www.asme.org/codes-standards/find-codes-standards/y14-5-dimensioning-tolerancing

[21] "ISO 10360-2:2009," ISO. Accessed: Feb. 16, 2025. [Online]. Available: https://www.iso.org/standard/40954.html

[22] "Leica Absolute Tracker AT960 | Hexagon." Accessed: Feb. 17, 2025. [Online]. Available: https://hexagon.com/products/leica-absolute-tracker-at960

[23] 7D Kinematic Metrology, "6th Generation Technology Further Increases iGPS Usability & Performance." Accessed: Feb. 17, 2025. [Online]. Available: https://7dkmetrology.com/7dk-1/i5is-en